Electronic structure of half-metallic ferromagnets and spinel ferromagnetic insulators

2004 J. Phys.: Condens. Matter 16 S5587

(http://iopscience.iop.org/0953-8984/16/48/015)

INSTITUTE OF PHYSICS PUBLISHING JOURNAL OF PHYSICS: CONDENSED MATTER

J. Phys.: Condens. Matter **16** (2004) S5587–S5600 PII: S0953-8984(04)83056-X

Electronic structure of half-metallic ferromagnets and spinel ferromagnetic insulators

Z Szotek[1], W M Temmerman[1], A Svane[2], L Petit[3], P Strange[4], G M Stocks[5], D Ködderitzsch[6], W Hergert[6] and H Winter[7]

[1] Daresbury Laboratory, Daresbury, Warrington WA4 4AD, Cheshire, UK
[2] Institute of Physics and Astronomy, University of Aarhus, DK-8000 Aarhus C, Denmark
[3] Computer Science and Mathematics Division, and Center for Computational Sciences, Oak Ridge National Laboratory, Oak Ridge, TN 37831, USA
[4] School of Chemistry and Physics, Keele University, Staffordshire ST5 5BG, UK
[5] Metals and Ceramics Division, Oak Ridge National Laboratory, Oak Ridge, TN 37830, USA
[6] Fachbereich Physik, Martin-Luther-Universität Halle-Wittenberg, Friedemann-Bach-Platz 6, D-06099 Halle, Germany
[7] INFP, Forschungszentrum Karlsruhe GmbH, Postfach 3640, D-76021 Karlsruhe, Germany

Received 29 June 2004, in final form 29 June 2004
Published 19 November 2004
Online at stacks.iop.org/JPhysCM/16/S5587
doi:10.1088/0953-8984/16/48/015

Abstract

We discuss an application of the self-interaction-corrected local spin density (SIC-LSD) approximation to study electronic structure of some half-metallic ferromagnets and ferromagnetic insulators of current interest in spintronics. Both d- and f-electron materials are considered, and we concentrate on the nominal valence and ground state properties of these systems.

(Some figures in this article are in colour only in the electronic version)

1. Introduction

The field of spintronics is concerned with the search for highly spin-polarized materials with the aim of enhancing the tunnelling magnetoresistance (TMR) of magnetic tunnel junctions (MTJs), which are active members of magnetic random access memory (MRAM) elements. Another goal is to increase the spin polarization of currents injected into semiconductors. There are two ways of achieving high spin polarization, namely by employing half-metals (HM) or by exploiting spin-filtering effects.

The half-metallic systems are generally referred to as half-metallic ferromagnets (HMFs). The concept of a half-metallic ferromagnet was introduced by de Groot *et al* [1], based on their electronic structure calculations for Heusler systems NiMnSb and PtMnSb. Half-metallic ferromagnets are solids that are metals with a Fermi surface in one spin channel, and insulators or semiconductors in the other spin channel. They give rise to 100% spin polarization at the Fermi energy, E_F, which makes them ideal materials for spin-dependent devices and

spin injection. A broad classification scheme of half-metallic ferromagnets, encompassing localized and itinerant electron systems as well as possible semimetals and semiconductors, was proposed by Coey and Venkatesan [2], based on the electronic structure.

All half-metals contain more than one element. Normal ferromagnets like Fe, Co and Ni are not half-metals. Although Co and Ni have fully spin-polarized d bands, with fully occupied majority spin states and only minority spin states at the Fermi level, the latter also crosses the unpolarized 4s band. So, there are both the spin-up and spin-down densities of states (DOSs) present at E_F. Most known half-metals are either oxides, sulfides, or Heusler alloys. Calculations also find some rare earth (RE) pnictides and chalcogenides to be half-metallic [3, 4]. Recently, half-metallic transition metal (TM) oxides have been the most actively studied half-metals. CrO_2 is the best known oxide half-metal with only spin-up electrons of mostly $Cr(t_{2g})$ character at the Fermi level. Another well known half-metal of the same type (IA) is the half-Heusler alloy NiMnSb, with only spin-up electrons of $Ni(e_g)$ character at E_F. The double-perovskite Sr_2FeMoO_6 is an example of a type IB half-metal [2], with no spin-up electrons at the Fermi level, but with the spin-down conduction electrons of strongly hybridized $Fe(3d_{t_{2g}})$, $Mo(4d_{t_{2g}})$, and O(2p) character. Magnetite belongs to the type II half-metals, where electrons lie in a band that is sufficiently narrow for them to be localized. The best indication of a type I or type II half-metal is metallic conduction in a solid, with a spin moment at $T = 0$ K which is precisely an integer number of Bohr magnetons (μ_B) per unit cell [2]. By virtue of integer filling of one spin channel in stoichiometric half-metals, the resulting spin magnetic moment per unit cell is also integer. The integer spin moment criterion is a necessary but not a sufficient condition for half-metallicity. Spin–orbit coupling may destroy half-metallicity [5].

The question of whether the total spin moment can be zero, whilst retaining half-metallicity, was addressed first by Leuken *et al* [6]. Not to be confused with usual antiferromagnets, they defined a half-metallic antiferromagnet (HMAF) as a half-metal with vanishing macroscopic spin moment. Half-metallic antiferromagnets would be ideal tip materials in spin-polarized STM (SPSTM) and could have important implications for superconductivity [7]. We shall show that some vacancy-doped TM oxides can become half-metals, and in particular NiO with about 3% of cation vacancies is a half-metal with zero spin magnetic moment, i.e., a half-metallic antiferromagnet [8].

Ferromagnetic insulators can very probably be used as spin filters of almost 100% spin filtering efficiency. The spin-dependent gap should result in a spin-dependent barrier for spin tunnelling of electrons through the insulator, giving rise to spin filtering. Since the tunnelling probability depends exponentially on the barrier height, the spin efficiency can be very high. The spin filtering effect has been demonstrated in Gd/EuS/Al junctions [9], which exhibit high magnetoresistance, but show no great prospects for technological applications, on account of the low T_c (16 K) of EuS. Also, EuO/Si(001) has been investigated as a possible spin filter. EuO is a semiconductor and it is one of the very rare ferromagnetic oxides. A ferromagnetic order sets in at $T_c = 69$ K. From their spin-polarized x-ray (XAS) absorption spectroscopy, Steeneken *et al* [10] concluded that electron-doped EuO in the ferromagnetic state will have almost 100% spin-polarized charge carriers. Other candidates for spin filters include such spinel materials as $NiFe_2O_4$ and $CoFe_2O_4$ [11]. Recently, Lüders *et al* [12] have obtained TMR of 120% in $La_{2/3}Sr_{1/3}MnO_3/SrTiO_3/NiFe_2O_4$ junctions, which corresponds to 42% spin polarization for the conductive $NiFe_2O_4$ film, which stays constant up to about 300 K.

The TM d electrons in oxides, as well as f electrons in RE compounds, are strongly correlated and cannot be adequately described within a standard band theory framework such as the local spin density (LSD) approximation to density functional theory (DFT). The self-interaction-corrected (SIC)-LSD [13], on the other hand, provides a better description of correlations than LSD, and has been successfully applied to a variety of d- and f-electron

materials [14–16]. An overview of the basic features of the SIC-LSD formalism is presented in the next section, whilst its applications to double perovskites Ba_2FeMoO_6, Ca_2FeMoO_6, Sr_2FeMoO_6, and Ca_2FeReO_6, magnetite, and a spinel ferromagnet $NiFe_2O_4$ are presented and discussed in section 3. There we also report on cation-vacancy-induced half-metallicity in MnO and NiO, and some RE compounds of possible interest for spintronics. The paper is concluded in section 4.

2. Theory

The basis of the SIC-LSD formalism is a self-interaction free total energy functional, E^{SIC}, obtained by subtracting from the LSD total energy functional, E^{LSD}, a spurious self-interaction of each occupied electron state ψ_α [17], namely

$$E^{\mathrm{SIC}} = E^{\mathrm{LSD}} - \sum_{\alpha}^{\mathrm{occ}} \delta_\alpha^{\mathrm{SIC}}. \tag{1}$$

Here α numbers the occupied states and the self-interaction correction for the state α is

$$\delta_\alpha^{\mathrm{SIC}} = U[n_\alpha] + E_{\mathrm{xc}}^{\mathrm{LSD}}[\bar{n}_\alpha], \tag{2}$$

with $U[n_\alpha]$ being the Hartree energy and $E_{\mathrm{xc}}^{\mathrm{LSD}}[\bar{n}_\alpha]$ the LSD exchange–correlation energy for the corresponding charge density n_α and spin density $\bar{n}_\alpha$. It is the LSD approximation to the exact exchange–correlation energy functional which gives rise to the spurious self-interaction. The exact exchange–correlation energy E_{xc} has the property that for any single electron spin density, $\bar{n}_\alpha$, it cancels exactly the Hartree energy, thus

$$U[n_\alpha] + E_{\mathrm{xc}}[\bar{n}_\alpha] = 0. \tag{3}$$

In the LSD approximation this cancellation does not take place, and for well localized states the above sum can be substantially different from zero. For extended states in periodic solids the self-interaction vanishes.

The SIC-LSD approach can be viewed as an extension of LSD in the sense that the self-interaction correction is only finite for spatially localized states, while for Bloch-like single-particle states E^{SIC} is equal to E^{LSD}. Thus, the LSD minimum is also a local minimum of E^{SIC}. The question now arises of whether there exist other competitive minima, corresponding to a finite number of localized states, which could benefit from the self-interaction term without losing too much of the energy associated with band formation. This is often the case for rather well localized electrons like the 3d electrons in transition metal oxides or the 4f electrons in rare earth compounds. It follows from minimization of equation (1) that within the SIC-LSD approach such localized electrons move in a different potential from the delocalized valence electrons which respond to the effective LSD potential. Thus, by including an explicit energy contribution for an electron to localize, the *ab initio* SIC-LSD describes both localized and delocalized electrons on an equal footing, leading to a greatly improved description of correlation effects over the LSD approximation, as well as to determination of valence.

In order to make the connection between valence and localization more explicit, it is useful to define the nominal valence [16] as

$$N_{\mathrm{val}} = Z - N_{\mathrm{core}} - N_{\mathrm{SIC}},$$

where Z is the atomic number (26 for Fe), N_{core} is the number of core (and semi-core) electrons (18 for Fe), and N_{SIC} is the number of localized, i.e., self-interaction-corrected, states (either five or six, respectively for Fe^{3+} and Fe^{2+}). Thus, in this formulation the valence is equal to the integer number of electrons available for band formation. The localized

Table 1. Total and element-decomposed spin magnetic moments (in μ_B) as calculated within SIC-LSD. In the last row the respective volumes per formula unit are quoted (in (atomic units)^3).

Moment	Ca_2FeReO_6	Ca_2FeMoO_6	Sr_2FeMoO_6	Ba_2FeMoO_6
M_{total}	3.00	4.00	4.00 (4.00)	4.00
M_{Fe}	3.87	3.76	3.71 (3.65)	3.81
M_{Mo}	—	−0.40	−0.43 (−0.35)	−0.41
M_{Re}	−1.12	—	—	—
M_{AE}	−0.02	0.01	0.02 (0.02)	0.02
M_{O1}	0.02	0.10	0.11 (0.11)	0.09
M_{O2}	0.01	0.11	0.11 (0.11)	—
M_{O3}	0.11	0.11	—	—
Volume	773.8	777.5	830.2	884.0

electrons do not participate in bonding. To find the nominal valence we assume various atomic configurations, consisting of different numbers of localized states, and minimize the SIC-LSD energy functional of equation (1) with respect to the number of localized electrons.

The SIC-LSD formalism is governed by the energetics due to the fact that for each orbital the SIC differentiates between the energy gain due to hybridization of the orbital with the valence bands and the energy gain upon localization of the orbital. Whichever wins determines if the orbital is part of the valence band or not, and in this manner also leads to the evaluation of the valence of elements involved. The SIC depends on the choice of orbitals and its value can differ substantially as a result of this. Therefore, one has to be guided by the energetics in defining the most optimally localized orbitals to determine the absolute energy minimum of the SIC-LSD energy functional. The advantage of the SIC-LSD formalism is that for such systems as transition metal oxides or rare earth compounds the lowest energy solution will describe the situation where some single-electron states may not be of Bloch-like form. Specifically, in RE compounds these will be REs 4f states and in oxides Mn, Ni, and Fe 3d states, but not the O 2p, Mo 4d, or Re 5d states, since treating them as localized is energetically unfavourable.

3. Results and discussion

3.1. Double perovskites

Interest in ordered double perovskites started with the discovery of the room-temperature colossal magnetoresistance (CMR) in Sr_2FeMoO_6 [18]. Experimentally, half-metallic behaviour in this compound is indicated by the observed high transition temperature T_c and low field magnetoresistance. In calculations, it is manifested through a well defined gap in the majority spin channel, and metallic behaviour in the minority spin channel, with strongly hybridized bands of Fe 3d(t_{2g}), Mo 4d(t_{2g}), and O 2p character at the Fermi level.

The SIC-LSD calculations find all the double perovskites presented in table 1 to have half-metallic ground state, with 100% spin-polarized conduction electrons [19]. The half-metallic character is reflected through the total spin magnetic moments, that are all integer. The spin moments induced by hybridization on the Mo sites of the various compounds are of similar magnitude, about $-0.4\ \mu_B$, independently of the alkaline earth (AE) element, while that of Re is of the order of $-1.1\ \mu_B$. These induced spin magnetic moments are antiparallel aligned with the Fe spin moment. It is interesting to note that the magnetic properties of these compounds seem unaffected by either the type of the alkaline earth atom, or the substantial change in their volumes. However, the calculated small reduction of the Mo spin moment in Ca_2FeMoO_6, in comparison with Sr_2FeMoO_6, has been confirmed in the recent NMR experiment of

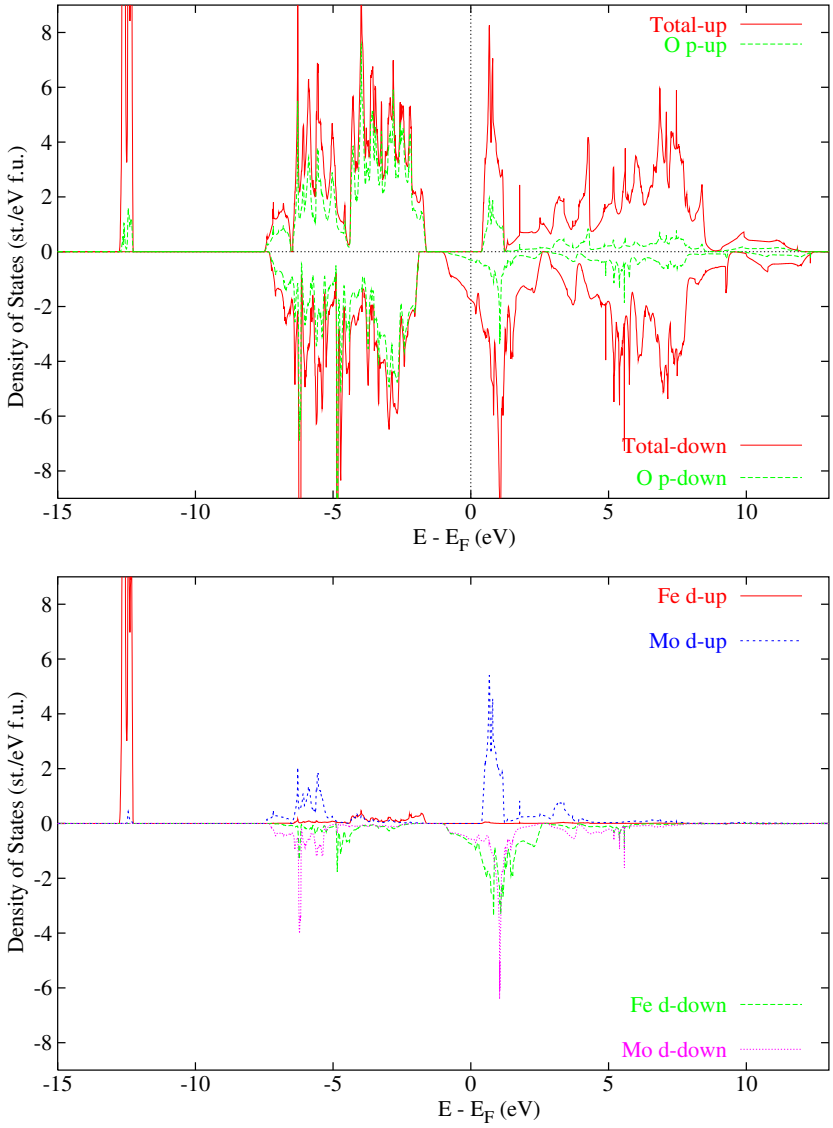

Figure 1. Spin-polarized total and oxygen 2p densities of states, per formula unit, for Sr_2FeMoO_6 (top), and spin-polarized Fe 3d and Mo 4d densities of states per formula unit (bottom). The minority DOS is printed on the negative side of the *y*-axis.

Wojcik *et al* [20]. Also, the reduction in the size of the Fe and Mo spin moments for Sr_2FeMoO_6, as a result of implementing theoretical optimization of oxygen positions, as given by Kobayashi *et al* [18], does not seem too important although it brings the size of our calculated spin moments (given in parenthesis in the fourth column of table 1) close to their values. The changes in the spin moments of the other species cannot be resolved when rounded off to two digits after the decimal point.

The spin-polarized ground state DOSs are very similar for all the compounds, independently of which alkaline earth compound is considered. In figure 1 we show the

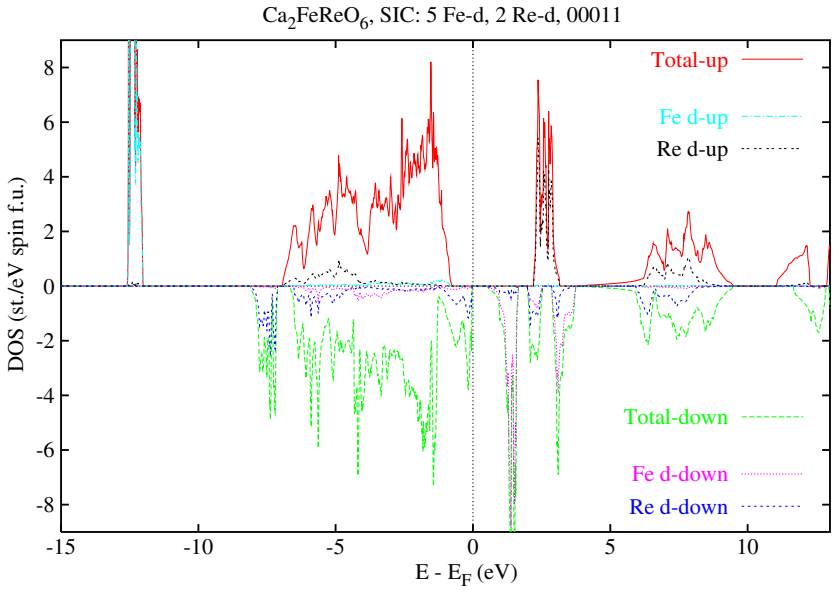

Figure 2. Spin-polarized total densities of states, per formula unit, for Ca_2FeReO_6 for the insulating solution that is 140 mRyd unfavourable with respect to the calculated half-metallic ground state. Also shown are Fe d and Re d contributions to the total DOS. The minority DOS is printed on the negative side of the *y*-axis.

spin-polarized DOS for Sr_2FeMoO_6, as a representative of the double perovskites studied. The DOSs show a convincing half-metallic behaviour, with a well defined gap at the Fermi energy in the majority spin channel, and strongly hybridized Fe 3d, Mo 4d, and oxygen 2p states in the other spin channel. In the ionic model for A_2FeMoO_6, where A = Ca, Sr, Ba, one would expect insulating behaviour due to the A^{2+}, Fe^{3+}, Mo^{5+}, and O^{2-} valencies. However, from the SIC-LSD calculations, we obtain an Fe^{3+}/Mo^{6+} ground state configuration (namely five localized Fe d electrons and six delocalized Mo d electrons), meaning that while 12 electrons fill up the O holes in both the majority and minority spin channels, the remaining one electron will partially fill the conduction bands, unoccupied in the insulating scenario. Half-metallicity results from the fact that, due to Fe–Mo–O hybridization, the conduction bands are exchange split, and therefore the one electron occupies the minority conduction bands only.

Also for Ca_2FeReO_6 we find the ground state to be half-metallic, rather than insulating, as suggested in [21]. The corresponding nominal valencies, Fe^{3+} and Re^{7+}, entail that in this case 8 out of 14 electrons fill the O p band in the minority spin channel plus some Fe and Re t_{2g} states. This is reflected in the total spin magnetic moment (table 1), which drops from 4 μ_B in Ca_2FeMoO_6 to 3 μ_B in Ca_2FeReO_6. Compared to the half-metallic ground state, the least unfavourable insulating state for Ca_2FeReO_6 has been obtained when treating five majority Fe 3d(Fe^{3+}) electrons and two minority Re 5d(Re^{5+}) electrons as localized. It has been unfavourable by 140 mRy with respect to the calculated SIC-LSD half-metallic ground state of this compound, the reason being that the loss in band formation energy upon localization of Re d electrons by far outweighs the gain in localization energy. In figure 2, we show the DOS for this insulating solution. Note that in this case the gap in the minority channel is much smaller than in the majority channel, and the system looks on the verge of transition to the half-metallic state. It seems that to get a stable insulating ground state for Ca_2FeReO_6 one

would need to consider other factors such as perhaps mis-site disorder, lattice relaxations, etc, which would involve large supercells for the calculations.

In summary, the half-metallic ground state seems to be a rather generic result for the double perovskites involving Fe with filled majority d shell, filled O p band, and Mo and Re transition metal ions which see their minority d bands occupied by one (Mo) to two (Re) electrons.

3.2. Fe_3O_4 and $NiFe_2O_4$

Based upon its high magnetoresistive properties, magnetite (Fe_3O_4) is also of interest for technological applications, e.g. computer memory, magnetic recording, etc. $NiFe_2O_4$ is a ferromagnetic insulator that is of possible interest as a spin filter in MTJs [11, 12]. Magnetite is thought to be half-metallic, with a highest known T_c of 860 K. Remarkably, at about $T_V = 122$ K it undergoes a transition to an insulating state, associated with some kind of charge order, setting in on the octahedral sites, and a distortion of the crystal structure from the inverse spinel cubic to monoclinic [22–24]. Verwey argued that below the transition temperature, T_V, the Fe^{3+} and Fe^{2+} cations order in the alternate (001) planes, and interpreted this transition as an electron localization–delocalization transition [22].

We have studied three different types of charge order on the octahedral sites, both in the high-temperature (cubic) and low-temperature (monoclinic) phases [25]. In particular, we considered the simple Verwey charge order (SIC(1)), the case where all the octahedral sites are occupied by Fe^{3+} (SIC(2)), and finally the scenario with all the octahedral sites occupied by the Fe^{2+} ions (SIC(3)) [25]. For all these scenarios the tetrahedral sites have been occupied only by Fe^{3+} ions. Our SIC-LSD total energy calculations, both for the cubic and monoclinic structures, have shown that not the Verwey phase, but the scenario with all interstitial, namely both the tetrahedral and octahedral, sites occupied by Fe^{3+}, is the ground state, followed by the Verwey phase (unfavourable by 113 mRyd in the cubic phase and 108 mRyd in the monoclinic phase), and then the all Fe^{2+} scenario. These significant total energy differences, found between scenario SIC(1) and scenario SIC(2) in both phases, have rendered the simple Verwey ordering highly unlikely as an explanation for the properties in the low-temperature phase of magnetite. Thus, if at all, the charge order must be much more complex than postulated by Verwey. Obviously we have studied only the three simplest charge order scenarios, and within these restrictions our results have indicated the energetically unfavourable character of Fe^{2+}. This does not exclude the possibility that Fe_3O_4 below the Verwey temperature is described by a much more complicated charge-ordered state.

In what follows we concentrate on the simple Verwey charge order solution for the cubic phase and in figure 3 compare its spin-resolved total densities of states with those for the ferromagnetic spinel insulator $NiFe_2O_4$. As seen in figure 3, top panel, in the Verwey phase, we have calculated magnetite to be insulating with a gap of $\sim$0.35 eV in the cubic phase ($\sim$0.1 eV in the monoclinic phase, which compares well with the experimental value of 0.14 eV [26]), while the all Fe^{3+} scenario has given rise to a half-metallic, ground state, solution [25]. The valence band is predominantly O p in character, while the sharp peaks below the valence band are due to the SIC localized TM 3d states. For $NiFe_2O_4$, we find an insulating solution in the inverse spinel structure, with an energy gap of about 1.2 eV, to be the ground state. Specifically, the octahedral sites are occupied by Ni^{2+} and Fe^{3+} ions, while the tetrahedral sites only by Fe^{3+} ions. Replacing the Fe^{2+} ions on the octahedral sites by Ni^{2+} leads to the reduction of the total spin magnetic moment of 4 μ_B in magnetite to 2 μ_B in $NiFe_2O_4$, since the spin magnetic moment of the Ni^{2+} ion is 1.57 μ_B, as compared to the 3.56 μ_B spin moment of the Fe^{2+} ion. The oxygen spin moments in both materials are comparable, of the order of 0.1 μ_B, and aligned in parallel to the cation spin moments on the octahedral sites. The width of the predominantly

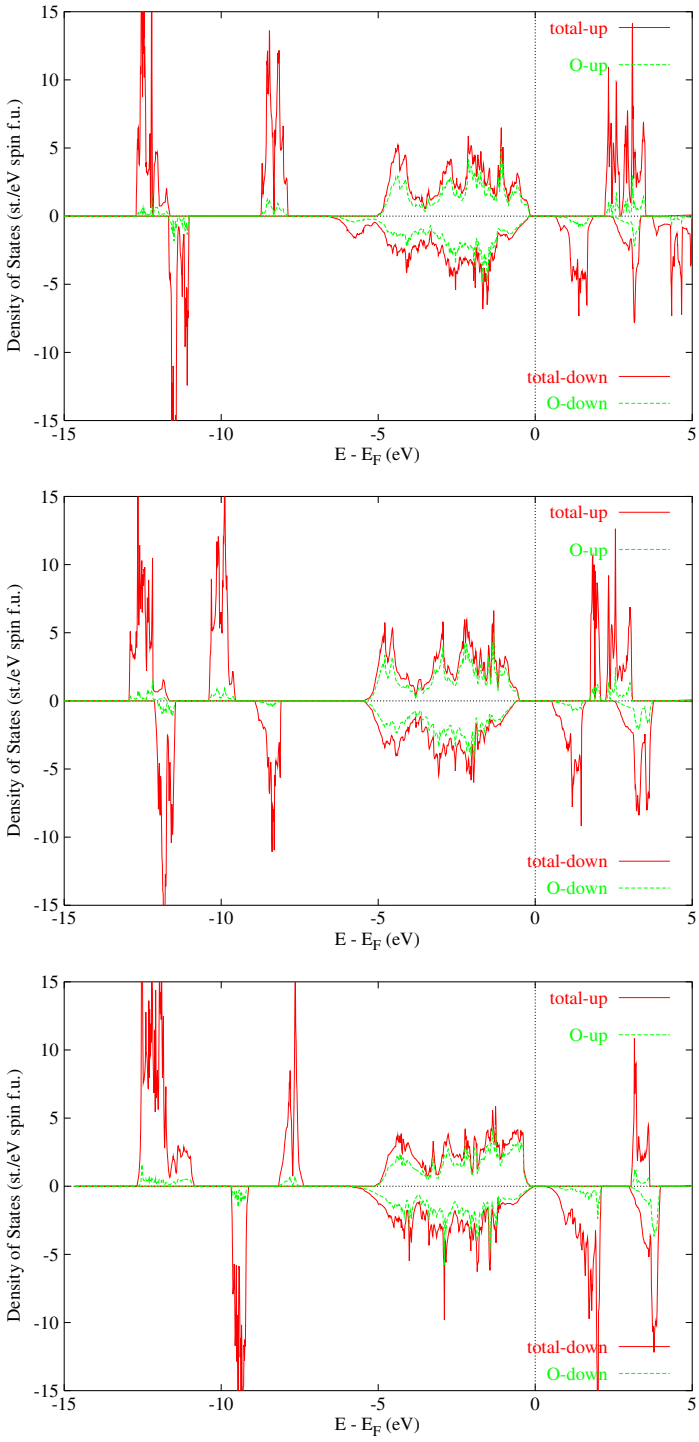

Figure 3. Spin-polarized total densities of states, per formula unit, for Fe_3O_4 in the inverse spinel structure (top), $NiFe_2O_4$ in the inverse spinel structure (middle), and $NiFe_2O_4$ in the normal spinel structure (bottom). The oxygen contribution to the total density of states is also shown. The minority DOS is printed on the negative side of the y-axis.

oxygen 2p valence band is reduced when moving from Fe_3O_4 to $NiFe_2O_4$, resulting from the fact that the sixth localized d electron of the Fe^{2+} ion, in figure 3 seen at the bottom of the valence band between -5.0 and -6.0 eV, is strongly hybridized with the oxygen p band. The situation is different in $NiFe_2O_4$, where the three localized minority t_{2g} electrons, seen at about -8.0 eV, are well separated from the bottom of the valence band. Also, the exchange splitting of the conduction band, of importance to spin filtering, is about 20% smaller in $NiFe_2O_4$ than in the Verwey phase of Fe_3O_4.

Since samples used in experiments usually contain a substantial amount of mis-site disorder [27], it is interesting to study the change in the electronic structure of $NiFe_2O_4$ in the extremal situation, namely in the normal spinel structure. In this case the Ni^{2+} ions occupy the tetrahedral sites, while the octahedral sites are solely taken by the Fe^{3+} ions. As a result, the total spin magnetic moment is increased from 2 μ_B per formula unit to 8 μ_B per formula unit, in agreement with experimental findings of [12]. However, as seen in the bottom panel of figure 3, the density of states is still just insulating in both spin channels, at variance with the experimental implications [12]. Also, unlike the case of the inverse spinel structure, the valence band is strongly spin polarized. The oxygen spin magnetic moment is 0.3 μ_B, aligned in parallel to the Fe spin moment, and three times the value it has in the inverse spinel structure. Also, the Ni spin moment is slightly increased to -1.65 μ_B. Moreover, the exchange splitting of the conduction band is increased more than twofold in the normal spinel, in comparison with the inverse spinel, structure. What is interesting is the fact that in realizing Ni^{2+} ions, the e_g states are populated first, i.e., are lying lower in energy than the t_{2g} states, as is the case for the inverse spinel structure. However, energetically, the normal spinel structure for $NiFe_2O_4$ is unfavourable with respect to the inverse spinel structure. Thus, our SIC-LSD calculations find $NiFe_2O_4$ to be an inverse spinel ferromagnetic insulator, at variance with magnetite for which we find a half-metallic ground state in both high-and low-temperature phases [25].

3.3. Vacancy-doped transition metal oxides

Recently, it has been predicted [28] that nonmagnetic insulating oxides, like CaO and MgO, in the rock-salt structure, can be made half-metallic upon introduction of a low concentration of vacancies on the cation sites. Here we show, based on first-principles SIC-LSD calculations, that introducing cation vacancies into antiferromagnetic insulating transition metal (TM) oxides not only leads to half-metallic behaviour, but in NiO a half-metallic antiferromagnetic state can be realized [8].

We have performed SIC-LSD *ab initio* calculations using a supercell approach to simulate the effect of placing cation vacancies in MnO and NiO [8]. The cubic supercell used in the calculations consists of 32 fu. To gain more insight, we have also studied in addition to the experimentally observed AF2 ordering, where spins are oppositely aligned in the subsequent (111) planes, a ferromagnetic (FM) alignment of spins. For the systems without vacancies, we have observed for both oxides insulating behaviour, with large bandgaps at the Fermi energy. The gaps are of charge transfer type—the top of the valence band is predominantly oxygen p-like, whereas the bottom of the conduction band is formed by transition metal d states. The oxygen p bands are not polarized in these AF2 bulk materials (see also [15]). For 3.125% of cation vacancies, introduced onto one spin sublattice (realizing $Mn_{0.97}O$ and $Ni_{0.97}O$), our calculations give half-metallic behaviour for both antiferromagnetic and ferromagnetic orders.

Table 2 shows the total spin magnetic moments of MnO and NiO without and with vacancies as calculated in the SIC-LSD supercell approach. In all the cases we obtain integer total spin magnetic moments. Most interestingly, a cation vacancy embedded into AF2-ordered NiO gives total spin magnetic moment of zero, i.e., this system is a half-metallic

Table 2. Total spin magnetic moments of the supercell with and without cation vacancy for both MnO and NiO. IS and HM denote insulating and half-metallic states, respectively.

System	Scenario	m^{total} (μ_{B})	State
MnO	AF2 no vacancy	0	IS
	AF2 with vacancy	3	HM
NiO	AF2 no vacancy	0	IS
	AF2 with vacancy	0	HM

antiferromagnet [6]. The spin moments given in table 2 imply that the spin polarization of neighbouring atoms, induced by vacancy creation, gives rise to a compensating integer spin moment of 2 μ_{B}, which in the case of NiO in the AF2 ordering makes the total spin moment exactly 0 μ_{B}. The way it comes about is because the oxygens around the cation vacancy in the AF2-NiO acquire a spin moment of 0.16 μ_{B} (in the system without vacancy the oxygens are frustrated in the AF2 ordering and have no spin moment), thus restoring the AF2 pattern, disturbed by taking out the Ni atom at the vacancy site. When comparing the spin moments on the Ni spheres to the respective bulk value of ± 1.56 μ_{B}, one realizes that the nearest Ni neighbours to the vacancy are essentially unaffected. However, the spin moments on the Ni next-nearest neighbours are decreased in magnitude by 0.07 μ_{B} compared to their values in the system without cation vacancy.

The vacancy induced half-metallicity of TM oxides survives a local 10% inward relaxation of the neighbouring oxygen atoms, but is lost when doubling the vacancy concentration on the same sublattice. The situation is the same when one removes a cation from each sublattice at the same time. In the present supercell approach this means that the two cation vacancies are placed so that both see the same environment, however with a reversed spin ordering. In this scenario, the half-metallicity is lost when considering the global picture; however, the spin polarization persists locally. Thus, if this local spin polarization were present at the surface, it could be detected by SPSTM.

3.4. Rare earth nitrides

There has been speculation in the literature that rare earth nitrides may form half-metallic ferromagnets [29–31]. If it is the case that they are half-metallic or narrow gap insulators then they have potential applications in spin filtering devices. There are severe technical barriers to the creation of such devices because the highest Curie temperature known for rare earth nitrides is about 60 K in GdN [32], well below the boiling point of nitrogen. However, devices have been fabricated with other rare earth compounds with low Curie temperatures such as EuS [9, 33] and EuSe [34, 35].

The magnetic structure of the rare earth nitrides is not always known. Only NdN, GdN, TbN and DyN definitely order ferromagnetically. SmN is known to be antiferromagnetic and to our knowledge most of the others have not been investigated in sufficient detail for their magnetic structure to be unambiguously known.

We have performed SIC-LSD calculations for all the rare earth nitrides, in the ferromagnetic ordering, in both the divalent and trivalent states [3]. Thus, in this study of rare earth nitrides we have been concerned with the nominal valence and ground state of these compounds. Table 3 shows the electronic properties of each material at the Fermi energy for the ground state configuration. It is clear from the table that most of the light rare earth nitrides are found to be half-metallic. Only CeN is metallic because it exists in the tetravalent state

Table 3. Spin-resolved bandgaps (in Ryd) and densities of states (in states/Rydberg/formula unit) at the Fermi energy for the rare earth nitrides.

	Bandgap		DOS	
Material	Spin-up	Spin-down	Spin-up	Spin-down
CeN	0	0	15.37	15.37
PrN	0	0.039	0.0001	0
NdN	0	0.065	0.068	0
PmN	0	0.076	31.77	0
SmN	0	0.095	154.56	0
EuN	0	0.107	69.85	0
GdN	0	0.082	0.065	0
TbN	0.008	0.052	0	0
DyN	0.018	0.058	0	0
HoN	0.031	0.004	0	0
ErN	0	0	0.682	69.57
TmN	0	0	1.52	220.78
YbN	0	0	1.72	93.18

Table 4. Total and species-decomposed spin magnetic moments (M_S) of the rare earth nitrides. All values are in Bohr magnetons (μ_B). The spin magnetic moments of empty spheres are not shown. The rare earth orbital moment (M_L) assumes that the rare earth ions obey Hund's rules.

	M_S			M_L
Material	RE	N	Total	RE
CeN	0.0	0.0	0.0	0.0
PrN	2.07	−0.08	2.00	−5.0
NdN	3.10	−0.11	3.00	−6.0
PmN	4.13	−0.14	4.00	−6.0
SmN	5.22	−0.24	5.00	−5.0
EuN	6.30	−0.30	6.00	−3.0
GdN	7.01	−0.04	7.00	−0.0
TbN	5.97	0.01	6.00	3.0
DyN	4.93	0.05	5.00	5.0
HoN	3.91	0.08	4.00	6.0
ErN	2.90	0.09	2.99	6.0
TmN	1.83	0.12	1.96	5.0
YbN	0.79	0.14	0.94	3.0

(in fact the trivalent state is also just metallic). TbN, DyN, and HoN are found to be narrow-gap insulators and ErN, TmN, and YbN are metallic in both spin channels.

The total and species-decomposed spin magnetic moments are displayed in table 4. There we also present the rare earth's orbital moments. With the exceptions of ErN, TmN, and YbN, the spin magnetic moments of these materials take on an integer value. This indicates that these systems are either insulating (Tb-, Dy-, and Ho-nitrides) or half-metallic (Pr- to Gd-compounds). CeN is a non-magnetic metal, and the last three compounds of the series are metallic in both spin channels. These results are as one would expect; the spin magnetic moment is dominated by the rare earth f electrons, with some hybridization yielding small contributions from the rare earth s–d electrons and the nitrogen p states. This indicates that the nitrogen p states occur in the same energy range as the valence rare earth states, allowing

Table 5. The bandgaps and the spin splitting, ΔE_{ex}, at the bottom of the conduction band for the europium chalcogenides. It is clear that the gap for the majority spin electrons is significantly smaller than the gap for the minority spin electrons. All energies are in eV.

	EuO		EuS		EuSe		EuTe	
	↑	↓	↑	↓	↑	↓	↑	↓
Gap	2.5	3.4	1.3	2.0	1.0	1.3	0.4	1.1
ΔE_{ex}	0.62		0.39		0.38		0.39	

hybridization to occur. It is interesting to note that the contribution from the nitrogen atom changes sign half way through the series, in which it follows the RE's orbital moment. It appears that the nitrogen moment wants to point antiparallel to the partially occupied f-spin channel.

The insulating (semiconducting), half-metallic and full metallic behaviours that we have calculated for RE nitrides seem to be a consequence of the N p and the bandlike rare earth f states occurring in the same energy window, in the vicinity of the Fermi level, which leads to strong hybridization of these states. Our results seem to suggest that rare earth nitrides and their alloys may enable us to fabricate materials with a wide and continuous range of useful properties, particularly with regard to spin filtering applications where they may provide alternatives to the rare earth chalcogenides already in use for this purpose [9, 33–35].

3.5. Eu compounds

As already mentioned, Eu chalcogenides might be of interest for spin filtering applications. Devices have been fabricated with Eu chalcogenides with low Curie temperatures such as EuS [9, 33] and EuSe [34, 35]. Thus, it is of interest to study the electronic structure of these compounds.

We have performed SIC-LSD calculations of the electronic structure for Eu chalcogenides in the rock-salt structure (most of the rare earth chalcogenides crystallize in this structure) and the ferromagnetic state for all the materials in both the divalent and trivalent states [4]. The lower total energy of the two states defines the stable valence and the ground state. Our calculations predict all the europium chalcogenides to be divalent and have semiconducting ground states. This is as we would have expected on simple shell-filling grounds.

As seen in table 5, the calculated bandgaps for the different spin channels are very different. Therefore, we have materials whose carriers will be more or less 100% spin-polarized in the ambient temperature range. In table 5 we also show for all the chalcogenides the calculated exchange splitting of the bottom of the conduction band. These results unambiguously confirm the recent experiments by Steeneken *et al* [10] which showed that EuO is a small-bandgap semiconductor and that in the ferromagnetic state the charge carriers are almost entirely in one spin direction. Steeneken *et al* estimate the exchange splitting in the conduction band of EuO as 0.6 eV, and we find our calculation in excellent agreement with this value. In addition, our SIC-LSD calculations suggest that there may be a range of temperatures for which this is true for all the europium chalcogenides in their ferromagnetic state. Furthermore these results have a clear implication that the bandgaps can be controlled by a careful choice of material and doping.

Steeneken *et al* [10] have also determined the x-ray absorption spectrum for EuO at the oxygen K-edge. They have shown that it is in good agreement with the density of states calculated with the LDA + U method with $U = 7.0$ eV. In figure 4, we show the spin-resolved

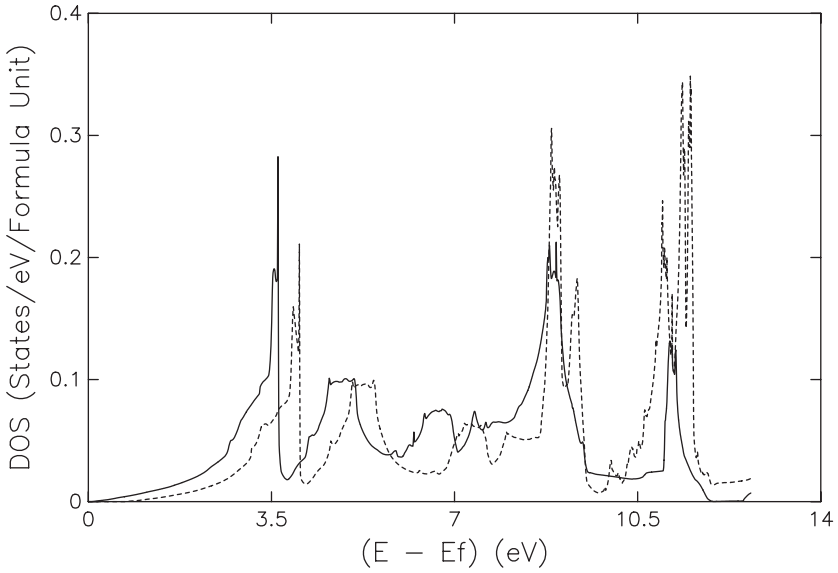

Figure 4. The unoccupied region of the oxygen p-resolved density of states for EuO. The full curve is for majority spin and the dashed curve for minority spin. The energies are relative to the Fermi energy, which is zero on this scale.

unoccupied p density of states on the oxygen site calculated with the SIC-LSD method which is completely first principles and exhibits good agreement with the XAS results. In the experiment the principal peaks occur at 532.5 eV with a shoulder at 534.5 eV and a double-peak structure at 536.0 and 538.0 eV. These features match well with our density of states peaks at 3.4, 5.0, 8.8 and 11.2 eV.

4. Conclusions

We have shown that, owing to a better treatment of correlations, SIC-LSD can provide useful insight into the nature of a variety of half-metallic materials. One can not only study their electronic and magnetic properties, but also such issues as valence and charge order. In particular, we have studied half-metals obtained by both electron and hole doping. The latter has been realized in the vacancy induced $Ni_{0.97}O$ and $Mn_{0.97}O$, where the carriers are predominantly O p, while the former occurs in the double perovskites and magnetite, where the carriers are mostly transition metal d electrons. Thus, it has been shown that SIC-LSD is a valuable tool for describing these new half-metals of high technological importance. Our calculations also show that the RE nitrides and europium chalcogenides may be possible candidates for spintronic and spin filtering applications.

Acknowledgments

This work has been partially funded by the Research Training Networks on 'Computational magnetoelectronics' (contract HPRN-CT-2000-00143) and '*Ab initio* computation of electronic properties of f-electron materials' (contract HPRN-CT-2002-00295). Partial sponsorship was also provided by the Defence Advanced Research Project Agency and the Division of Materials Sciences and Engineering, Office of Basic Energy Sciences,

US Department of Energy, under contract DE-AC05-00OR22725 with UT-Battelle LLC. M Horne and C M Aerts are gratefully acknowledged for giving us access to their results for rare earth compounds.

References

[1] de Groot R A, Mueller F M, van Engen P G and Buschow K H J 1983 *Phys. Rev. Lett.* **50** 2024
[2] Coey J M D and Venkatesan M 2002 *J. Appl. Phys.* **91** 8345
[3] Aerts C M, Strange P, Horne M, Temmerman W M, Szotek Z and Svane A 2004 *Phys. Rev.* B **69** 045115
[4] Horne M, Strange P, Temmerman W M, Szotek Z, Svane A and Winter H 2004 *J. Phys.: Condens. Matter* **16** 5061
[5] Eschrig H and Pickett W E 2001 *Solid State Commun.* **118** 123
[6] van Leuken H and de Groot R A 1995 *Phys. Rev. Lett.* **77** 1171
[7] Pickett W E 1996 *Phys. Rev. Lett.* **77** 3185
[8] Ködderitzsch D, Hergert W, Szotek Z and Temmerman W M 2003 *Phys. Rev.* B **68** 125114
[9] LeClair P, Ha J K, Swagten H J M, van de Vin C H, Kohlhepp J T and de Jonge W J M 2002 *Appl. Phys. Lett.* **80** 625
[10] Steeneken P G, Tjeng L H, Elfimov I, Sawatzky G A, Ghiringhelli G, Brookes N B and Huang D-J 2002 *Phys. Rev. Lett.* **88** 047201
[11] Pénicaud M, Siberchicot B, Sommers C B and Kübler J 1992 *J. Magn. Magn. Mater.* **103** 212
[12] Lüders U, Barthélémy A, Bibes M, Bouzehouane K, Jacquet E, Contour J-P, Fusil S, Bobo J-F, Fontcuberta J and Fert A 2004 *Appl. Phys. Lett.* submitted
[13] Temmerman W M, Svane A, Szotek Z and Winter H 1998 *Electronic Density Functional Theory: Recent Progress and New Directions* ed J F Dobson, G Vignale and M P Das (New York: Plenum)
[14] Svane A and Gunnarsson O 1990 *Phys. Rev. Lett.* **65** 1148
[15] Szotek Z, Temmerman W M and Winter H 1993 *Phys. Rev.* B **47** 4029
[16] Strange P, Svane A, Temmerman W M, Szotek Z and Winter H 1999 *Nature* **399** 756
[17] Perdew J P and Zunger A 1981 *Phys. Rev.* B **23** 5048
[18] Kobayashi K-I, Kimura T, Sawada H, Terakura K and Tokura Y 1998 *Nature* **395** 677
Kobayashi K-I, Kimura T, Sawada H, Terakura K and Tokura Y 1999 *Phys. Rev.* B **59** 11159
[19] Szotek Z, Temmerman W M, Svane A, Petit L and Winter H 2003 *Phys. Rev.* B **68** 104411
[20] Wojcik M, Jedryka E, Nadolski S, Rubi D, Frontera C, Fontcuberta J, Jurca B, Dragoe N and Berthet P 2004 *Preprint* cond-mat/0406161
[21] Gopalakrishnan J, Chattopadhyay A, Ogale S B, Venkatesan T, Greene R L, Millis A J, Ramesha K, Hannoyer B and Marest G 2000 *Phys. Rev.* B **62** 9538
[22] Verwey E J W and Haayman P W 1941 *Physica* **8** 979
Verwey E J W, Haayman P W and Romeijan F C 1947 *J. Chem. Phys.* **15** 181
[23] Walz F 2002 *J. Phys.: Condens. Matter* **14** R285
[24] Wright J P, Attfield J P and Radaelli P G 2001 *Phys. Rev. Lett.* **87** 266401
[25] Szotek Z, Temmerman W M, Svane A, Petit L, Stocks G M and Winter H 2003 *Phys. Rev.* B **68** 054415
[26] Park S K, Ishikawa T and Tokura Y 1998 *Phys. Rev.* B **58** 3717
[27] Bibes M 2004 private communication
[28] Elfimov I S, Yunoki S and Sawatzky G A 2002 *Phys. Rev. Lett.* **89** 216403
[29] Birgeneau R J, Bucher E, Passell L and Turberfield K C 1971 *Phys. Rev.* B **4** 718
[30] Kaldis E, Schulthess G V and Wachter P 1975 *Solid State Commun.* **17** 1401
[31] Hasegawa A and Yanase A 1977 *J. Phys. Soc. Japan* **42** 492
[32] Xiao J Q and Chien C L 1996 *Phys. Rev. Lett.* **76** 1727
[33] Filip A T, LeClair P, Smitts C J P, Koelhepp J T, Swagten H J M, Koopmans B and de Jonge W J M 2002 *Appl. Phys. Lett.* **81** 1815
[34] Worledge D C and Geballe T H 2000 *J. Appl. Phys.* **88** 5277
[35] Moodera J S, Meservey R and Hao X 1993 *Phys. Rev. Lett.* **70** 853